J. Cent. South Univ. (2018) 25: 1888−1894
DOI: https://doi.org/10.1007/s11771-018-3878-5

Springer

An investigation on crystallization property, thermodynamics and kinetics of wollastonite glass ceramics

SI Wei(司伟)[1], DING Chao(丁超)[2]

1. School of Materials Science and Engineering, Dalian Jiaotong University, Dalian 116028, China;
2. Dalian Environmental Monitoring Center, Dalian 116023, China

Abstract: Wollastonite glass ceramics were prepared using the reactive crystallization sintering method by mixing waste glass powders with gehlenite. The crystallization property, thermodynamics, and kinetics of the prepared wollastonite glass ceramics were determined by X-ray diffraction analysis, scanning electron microscopy, energy-dispersive spectroscopy, high-resolution transmission electron microscopy, and differential thermal analysis. Results showed that crystals of wollastonite and alumina could be found in the gehlenite through its reaction with silicon dioxide. The wollastonite crystals showed a lath shape with a certain length-to-diameter ratio. The crystals exhibited excellent bridging and reinforcing effects. In the crystallization process, the aluminum ions in gehlenite diffused into the glass and the silicon ions in the glass diffused into gehlenite. Consequently, the three-dimensional frame structure of gehlenite was partially damaged to form a chain-like wollastonite. The results of crystallization thermodynamics and kinetics indicated that crystallization reaction could occur spontaneously under a low temperature (1173 K), with 20 wt% gehlenite added as the reactive crystallization promoter. The crystallization activation energy was evaluated as 261.99 kJ/mol by using the Kissinger method. The compression strength of the wollastonite glass ceramic samples (7.5 cm×7.5 cm) reached 251 MPa.

Key words: glass ceramics; crystallization thermodynamics; crystallization kinetics

Cite this article as: SI Wei, DING Chao. An investigation on crystallization property, thermodynamic and kinetics of wollastonite glass ceramics [J]. Journal of Central South University, 2018, 25(8): 1888–1894. DOI: https://doi.org/10.1007/s11771-018-3878-5.

1 Introduction

Wollastonite glass ceramic is a new type of building decoration material that exhibits high intensity, attractive color, and no radioactivity [1–3]. It is usually prepared by melt crystallization, controlling different temperatures of the mother phase glass with the different chemical composition [4–7]. JANG et al [8] melted the parent material at 1863 K and prepared $0.9Ca_{0.9}Mg_{0.1}SiO_3$-$0.1CaMgSi_2O_6$ glass ceramics under different temperatures. SALMAN et al [9] used Na_2O-K_2O-CaO-SiO_2-F glass as the parent phase, melted it at 1673 K to 1723 K, annealed it at 773 K, and preserved the temperature for 1 h to obtain glass ceramics with biological activity, whose main crystal phase was wollastonite. YOON et al [10] mixed fly ash and waste glass, melted the mixture at 1673 K, quenched it with water at room temperature, and heat-treated it under different temperatures to obtain wollastonite glass ceramics.

Foundation item: Project(51308086) supported by the National Natural Science Foundation of China; Project(LJQ2015020) supported by the Program for Liaoning Excellent Talents in University, China; Project(2016RQ051) supported by the Program of Science-Technology Star for Young Scholars by the Dalian Municipality, China
Received date: 2017−03−27; **Accepted date:** 2017−07−18
Corresponding author: SI Wei, PhD, Associate Professor; Tel: +86–411–84107583; E-mail: siwei@djtu.edu.cn; ORCID: 0000-0002-8348-3970

Wollastonite glass ceramics prepared via melting are applied to bioactive materials, such as plasma-spraying apatite-wollastonite glass ceramic on the surface of titanium alloy [11] and apatite-wollastonite bioactive glass ceramic [12].

Local and foreign researches on waste glass focus mainly on manufacturing building materials, such as glass mosaic, artificial marble, foam glass, and wall and floor tiles, or replacing ceramic materials, such as feldspar and clay, with waste glass to preserve mineral resources [13–15]. Glass ceramic preparation that involves waste glass, fly ash, and volcanic ash using the solid phase sintering method is being increasingly adopted [16–17]. ABBASI et al [18] used soda–lime waste glass as a raw material to prepare glass ceramics with biological activity via solid-phase reaction.

Our research group used waste glass as a raw material to prepare a series of glass ceramic materials, such as wollastonite and fluorine amphibole, via the reactive crystallization sintering method [19−23]. This method does not require melting the glass with specific components, which is highly significant for conserving energy, reducing emissions, developing a circular crystallization mechanism of this method requires further research.

In the current study, wollastonite glass ceramics were prepared using the reactive crystallization sintering method. The crystallization property of wollastonite was studied, and thermodynamic and kinetic calculations were performed for the crystallization process to explore the inherent law of crystal transformation.

2 Experiment

2.1 Synthesis

The components of the waste window glass powder were 71.8 wt% SiO_2, 9.5 wt% CaO, 12.9 wt% Na_2O, 0.9 wt% Al_2O_3, 4.6 wt% MgO, and 0.3 wt% K_2O. Waste glass was washed, crushed, ground, and screened through a 120-mesh sieve (mesh size: 125 μm). Subsequently, 20 wt% gehlenite ($Ca_2Al_2SiO_7$) and a suitable amount of polyvinyl alcohol aqueous solution were added to the glass powder and mixed evenly to prepare round biscuits (φ 40 mm×5 mm) under 7.5 MPa pressure. The biscuits were then sintered at different temperatures (1073, 1123, 1173, 1223, and 1273 K) for different heat preservation time (0, 1, 2 and 4 h). A layer of gehlenite powder was sandwiched between two layers of glass powder to prepare the sandwich sample according to the aforementioned steps.

2.2 Characterization

A Rigaku D_{MAX}-12 X-ray diffractometer was used to determine the crystalline structure of the glass ceramic under the following conditions: voltage 40 kV, pipe flow 10 mA, and Cu K_α radiation (λ=0.15406 nm). An Oxford-INCA spectrum analyzer was used to analyze the changes in the elemental contents at the interface of gehlenite and glass of the sandwich samples at an accelerating voltage of 20 kV. A JEM-2100F high-resolution transmission electron microscope was used to observe the morphology of the samples at an accelerating voltage of 200 kV. An STA449F3 simultaneous thermal analyzer was used to measure the differential thermal analysis (DTA) curves of the samples (10 mg per sample) from 1170 K to 1263 K at heating rates of 5, 10, 15, and 20 K/min in argon flow of 100 mL/min.

3 Results and discussion

3.1 Phase analysis

The effect of different sintering temperatures on the phase structure of the glass ceramic was investigated, and the results are shown in Figure 1. The figure indicates that after being sintered at 1073 K, the main crystalline phase in the samples is gehlenite, whereas the precipitated secondary crystalline phases are wollastonite and small amounts of alumina. The figure also shows that the added gehlenite has partially reacted with the glass powders at this time to produce wollastonite and alumina. As the sintering temperature increased, the amount of produced wollastonite gradually increased and the main crystalline phase became wollastonite. This result indicated that rising temperature promoted reactive crystallization.

The effect of different heat preservation times at the sintering temperature of 1173 K on the phase structure of glass ceramic was investigated, and the results are shown in Figure 2. As can be seen in the figure, if heating was stopped immediately when the sintering temperature reached 1173 K or if the heat preservation time was 0, then the main crystalline phase of the samples became

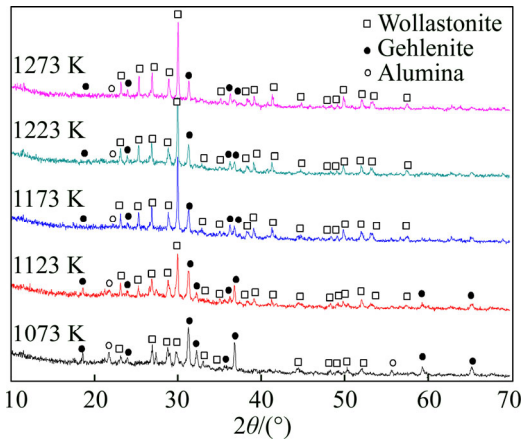

Figure 1 XRD profiles of glass ceramics prepared at different sintering temperature

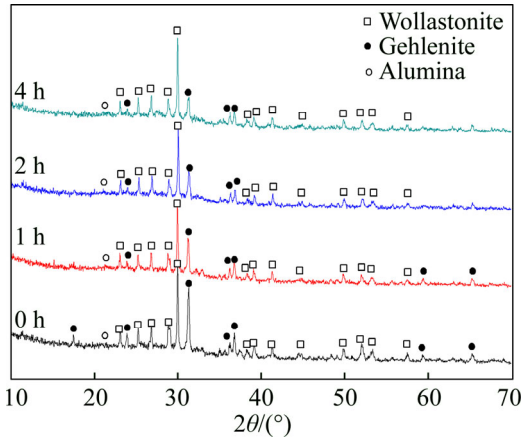

Figure 2 XRD profiles of glass ceramics prepared with different heat preservation times

wollastonite as the furnace cooled. However, the relative content of gehlenite increased. This result indicated that gehlenite did not undergo reactive crystallization completely with the glass powders. When the heat preservation time was 2 h, most of the gehlenite underwent reactive crystallization with the glass powders and achieved balance. When the heat preservation time was increased to 4 h, the content of gehlenite did not continuously reduce. This result indicated that preserving heat for 2 h was suitable.

3.2 Morphology and energy spectrum analysis

The scanning electron microscopy (SEM) photographs of the glass ceramics prepared with different heat preservation time are shown in Figure 3. As shown in the figures, when the heat preservation time was 0, an evident interface was formed between the glass and gehlenite and holes existed on the glass surface; moreover, granular crystals clearly appeared in the holes (Figure 3(a)). The waste glass used in the experiment exhibited extremely weak crystallization capability. Thus, crystallization was impossible. The outcome indicated that reactive crystallization of glass occurred between the glass and gehlenite. The X-ray diffraction (XRD) profile of the glass ceramic prepared with a heat preservation of 0 h also verified this finding.

When the heat preservation time was extended, the glass moved toward gehlenite via viscous flow. At this time, the interface between the glass and gehlenite was not evident. Instead, a transition layer with a certain thickness was formed. The thickness of the transition layer increased with heat preservation time (Figures 3(b)–(d)). When the heat preservation time was 2 h, the viscous flow resulted in the densification of the glass ceramic with holes on the surface. The crystallized wollastonite crystals exhibited a lath structure with a certain length-to-diameter ratio. The crystals demonstrated excellent bridging effect. The glass and the crystalline phases were in contact and formed an interlock structure.

Energy spectrum analysis was conducted on P_1, P_2, P_3, and P_4 (Figure 3) of the transition layer near gehlenite during the heat preservation process, as shown in Table 1. The results indicated that compared with the aluminum content of P_1 with a heat preservation time of 0, the aluminum contents of P_2, P_3 and P_4 decreased with prolonged heat preservation time. However, the silicon contents increased significantly. This result indicated that the Al^{3+} ions in gehlenite diffused into the glass and the Si^{4+} ions in the glass diffused into gehlenite during reactive crystallization.

High-resolution transmission electron microscopy (HRTEM) analysis was conducted on the glass ceramic that was sintered at 1173 K with a heat preservation time of 2 h, and the photograph is shown in Figure 4. Figure 4(a) presents the transmission electron microscopy (TEM) photograph. The figure indicates that the crystallized wollastonite crystals have a long cylindrical shape. The diffraction pattern shows that the crystallized crystals are single crystals. Figure 4(b) shows clear $(\bar{1}30)$ crystal stripes of wollastonite crystallized in the glass substrate, which demonstrate good crystallization.

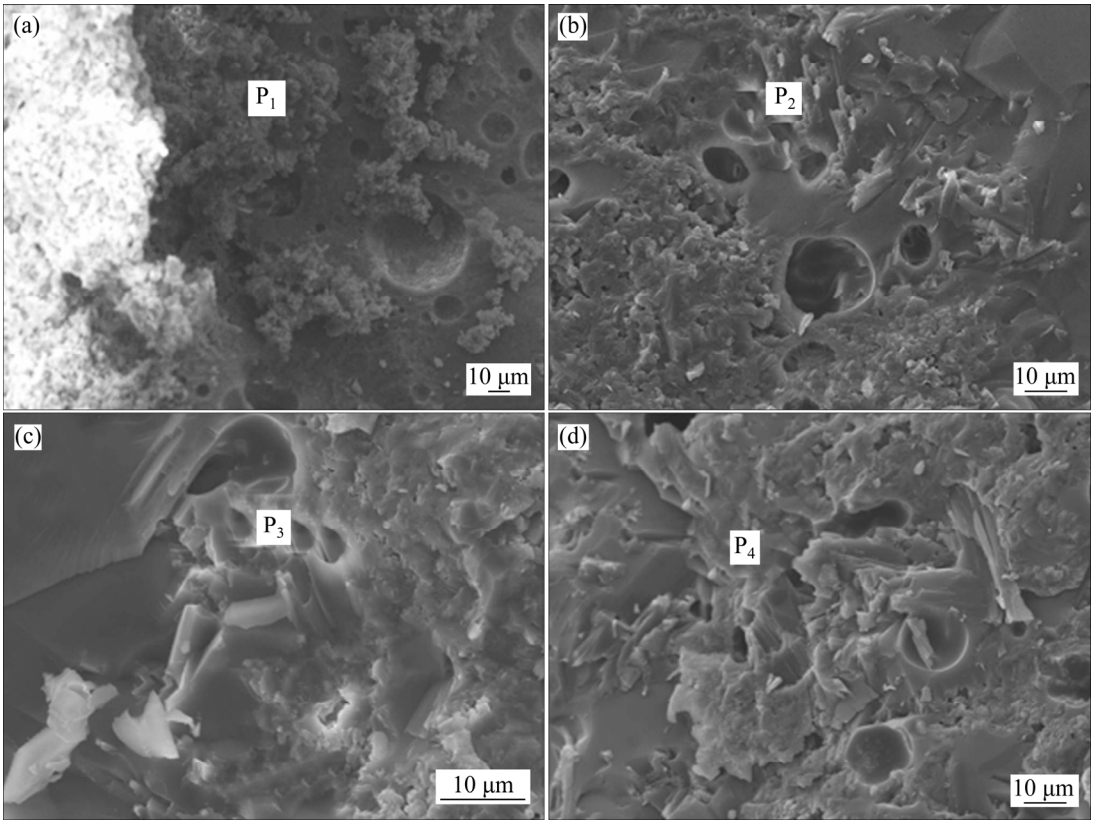

Figure 3 SEM photographs of glass ceramics with different heat preservation time: (a) 0 h; (b) 1 h; (c) 2 h; (d) 4 h

Table 1 Element contents at interface between gehlenite and glass in the holding process

Element	Mass fraction/%			
	0	1 h	2 h	3 h
O	54.89	46.56	47.96	50.11
Na	4.39	5.91	4.19	4.86
Mg	0.15	0.48	0.41	0.83
Al	**9.82**	**5.68**	**2.07**	**1.28**
Si	**9.34**	**17.36**	**22.95**	**25.57**
K	0.06	0.47	0.38	0.38
Ca	21.36	23.54	22.05	16.98
Total	100.00	100.00	100.00	100.00

3.3 Crystallization mechanism

Figure 5 presents the crystal structure diagrams of gehlenite and wollastonite, where the lattice parameters of gehlenite are a_G=0.769, b_G=0.769, c_G=0.510, and $\alpha=\beta=\gamma=90°$, and those of wollastonite are a_W=1.010, b_W=1.105, c_W=0.730, α=99.5°, β=100.5°, and γ=84.4°. The results of XRD, energy-dispersive X-ray spectroscopy, and HRTEM of the glass ceramic during the sintering process show that the Al^{3+} ions in gehlenite diffused into the glass and the Si^{4+} ions in the glass diffused into gehlenite. Oxygen replaced the $[Al_2Si_2]$ aluminum tetrahedron in gehlenite to form a $[SiO_4]$ tetrahedron. Ion movement damaged the 3D frame structure in gehlenite. At this time, $[CaO_6]$ octahedrons formed a single chain through common edge connection and the double oxygen–silicon tetrahedrons staggered with single silicon–oxygen tetrahedrons to form another single chain with $[Si_3O_9]$ as the structural unit [24]. The composite single chain formed by the two chains constitutes the wollastonite structural unit. Therefore, $b_G \approx c_W$ and $2c_G \approx a_W$.

The following reaction may occur during the reactive crystallization process:

$$Ca_2Al_2SiO_7 + SiO_2 \rightarrow 2CaSiO_3 + Al_2O_3 \quad (1)$$

3.4 Crystallization thermodynamic analysis

The standard molar enthalpy of formation of the oxides and the Gibbs free energy function of the substances can be obtained from the Practical Handbook of the Thermodynamics of Inorganic Materials, as shown in Table 2.

The Φ'_{1173} of the substances at 1173 K can be calculated based on Φ'_{1100} and Φ'_{1200} presented in the table using the following formula:

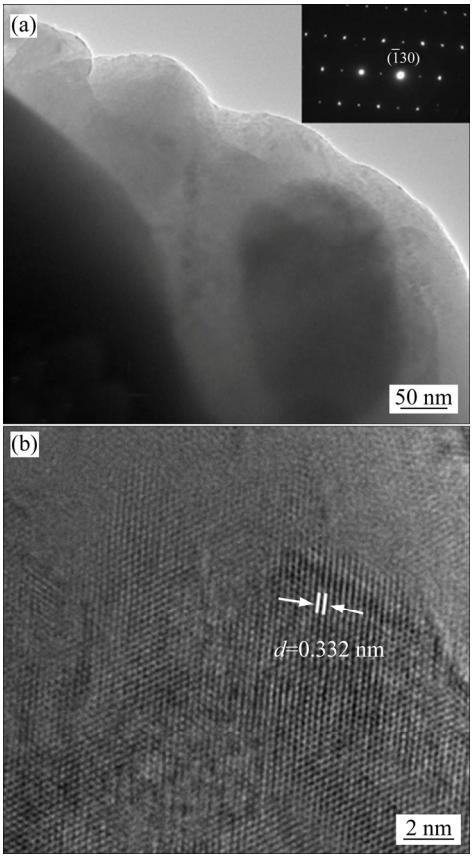

Figure 4 TEM photograph and embedded selected area electron diffraction pattern (a) and HRTEM photograph of wollastonite glass ceramics (b)

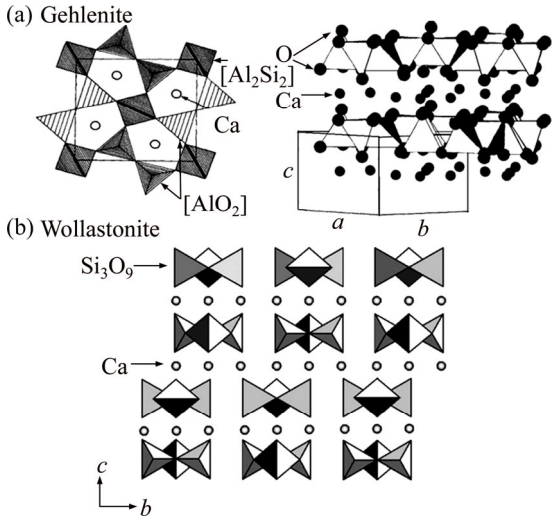

Figure 5 Crystal structure diagrams of gehlenite and wollastonite

$$\Phi'_{M,1173}=\Phi'_{M,1100}+\frac{\Phi'_{M,1173}-\Phi'_{M,1173}}{1200-1100}(1173-1100) \quad (2)$$

On the basis of the Gibbs–Helmholtz or Van't Hoff equation,

$$\Delta G^{\Theta}_{T}=\Delta H^{\Theta}_{298}-T\Delta\Phi'_{T} \quad (3)$$

Table 2 Standard molar enthalpy of formation and Gibbs free energy function of oxides

Compound	$\Delta H^{\Theta}_{f,298}$ / (kJ·mol^{-1})	Φ'_{1100} / (J·K·mol^{-1})	Φ'_{1200} / (J·K·mol^{-1})	Φ'_{1173}/ (J·K·mol^{-1})
$Ca_2Al_2SiO_7$	–3904.509	330.111	347.976	343.152
SiO_2	–847.260	79.225	83.271	82.179
$CaSiO_3$	–1634.270	142.545	149.916	147.926
Al_2O_3	–1675.274	109.770	117.084	115.109

On the basis of the crystallization equation, i.e., Eq. (1), the Gibbs free energy of the standard reaction is calculated by using Eq. (3) as follows:

$$\Delta H^{\Theta}_{298}=2\Delta H^{\Theta}_{f,298,CaSiO_3}+\Delta H^{\Theta}_{f,298,Al_2O_3}-\Delta H^{\Theta}_{f,298,Ca_2SiO_7}-\Delta H^{\Theta}_{f,298,SiO_2}=2(-1634.270)+(-1675.274)-(-3904.509)-(-847.260)=-192.045 \text{ kJ/mol}$$

$$\Delta\Phi'_{1173}=\sum(n_i\Phi'_{i,1173})_{Resultant}-\sum(n_i\Phi'_{i,1173})_{Reactants}=2(147.926)+(115.109)-(343.152+82.179)=-14.37 \text{ J/(K·mol)}$$

$$\Delta G^{\Theta}_{1173}=\Delta H^{\Theta}_{298}-T\Delta\Phi'_{1173}=-175.189 \text{ kJ/mol}$$

$$\Delta G_{1173}=\Delta G^{\Theta}_{1173}<0$$

Given that $\Delta G<0$, the crystallization reaction can occur spontaneously at 1173 K with gehlenite as the promoter to produce wollastonite glass ceramics.

3.5 Crystallization kinetic analysis

Figure 6 presents the DTA curves of the mixture of gehlenite and glass powders measured at the heating rates of 5, 10, 15 and 20 K/min. The figure shows that the mixed powders exhibit an evident crystallization exotherm in the heating process with crystallization exotherms, T_p, of 1172.032, 1202.357, 1219.297 and 1230.829 K, respectively.

Glass crystallization kinetics was analyzed based on the Johnson–Mehl–Avrami (JMA) state transition kinetics equation [25]. On the basis of the Kissinger equation,

$$\ln(T_p^2/\alpha)=E_a/RT_p+\ln(E_a/R)-\ln A \quad (4)$$

where α is the heating rate.

Relation diagram between $\ln(T_p^2/\alpha)$ and $1/T_p$ is indicated in Figure 7. The reactive crystallization

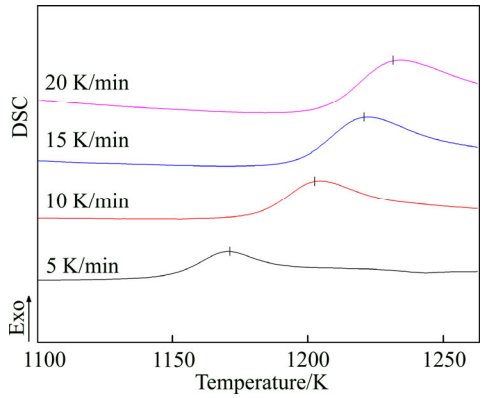

Figure 6 DTA curves of glass ceramics under different heating rates

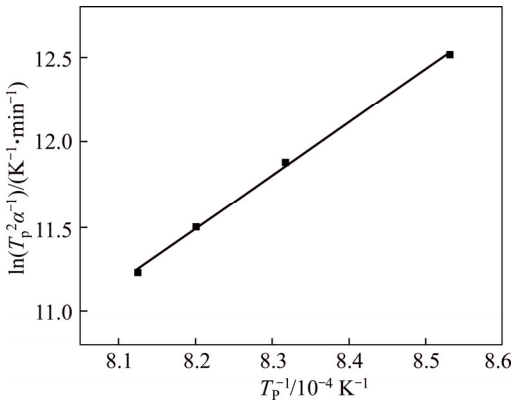

Figure 7 Relationship diagram between $\ln(T_p^2/\alpha)$ and $1/T_p$

activation energy can be calculated according to the slope $k= E_a/R$, where E_a=261.99 kJ/mol.

3.6 Mechanical property analysis

The wollastonite glass ceramic samples with dimensions of 7.5 cm×7.5 cm were prepared using a mold, as shown in Figure 8. The figure indicates that the samples exhibit a compact structure and a smooth surface. The mechanical property test shows that the compression strength is 251 MPa.

4 Conclusions

A wollastonite glass ceramic was prepared with waste glass added gehlenite by the reactive crystallization sintering method. Wollastonite and alumina crystals were found in gehlenite through its reaction with SiO_2. The wollastonite crystals were lath-shaped, exhibited bridging effect, and performed transportation and reinforcing roles. In the crystallization process, the aluminum ions in gehlenite diffused into the glass and the silicon ions in the glass diffused into gehlenite, which damaged the 3D frame structure of gehlenite to form a chain-like wollastonite. The crystallization reaction could occur spontaneously at 1173 K, with 20 wt% gehlenite added as the reactive crystallization promoter. The JMA formula indicated that the crystallization activation energy calculated using the Kissinger method was 261.99 kJ/mol. In addition, the compression strength of the wollastonite glass ceramic samples (7.5 cm×7.5 cm) reached 251 MPa. The reactive crystallization mechanism of silicate glass ceramics is also discussed.

Figure 8 Photograph of wollastonite glass ceramics

References

[1] FIOCCO L, ELSAYED H, DAGUANO J K M F, SOARES V O, BERNARDO E. Silicone resins mixed with active oxide fillers and Ca-Mg silicate glass as alternative/integrative precursors for wollastonite-diopside glass-ceramic foams [J]. Journal of Non-Crystalline Solids, 2015, 416: 44–49.

[2] TEIXEIRA S R, SOUZA A E, CARVALHO C L, REYNOSO V C S, ROMERO M, RINCON J M. Characterization of a wollastonite glass-ceramic material prepared using sugar cane bagasse ash (SCBA) as one of the raw materials [J]. Materials Characterization, 2014, 98: 209–214.

[3] KAMITAKAHARA M, OHTSUKI C, INADA H, TANIHARA M, MIYAZAKI T. Effect of ZnO addition on bioactive CaO-SiO_2-P_2O_5-CaF_2 glass-ceramics containing apatite and wollastonite [J]. Acta Biomaterialia, 2006, 2(4): 467–471.

[4] MOHAMMADI M, ALIZADEH P, ATLASBAF Z. Effect of frit size on sintering, crystallization and electrical properties of wollastonite glass-ceramics [J]. Journal of Non-Crystalline Solids, 2011, 357: 150–156.

[5] PARK J, YOU S H, SHIN D W, OZTURK A. Tribological behavior of alumina-added apatite-wollastonite glass-ceramics in simulated body fluid [J]. Materials Chemistry & Physics, 2010, 124(1): 113–119.

[6] KANSAL I, TULYAGANOV D U, GOEL A, PASCUAL M J, FERREIRA J. Structural analysis and thermal behavior of diopside-fluorapatite-wollastonite-based glasses and glass-

ceramics [J]. Acta Biomaterialia, 2010, 6: 4380–4388.
[7] TIAN Zhong-liang, YANG Kai, LAI Yan-qing, ZHANG Kai, LI Jie. Effect of sintering atmosphere on corrosion resistance of $NiFe_2O_4$ ceramic in Na_3AlF_6-Al_2O_3 melt [J]. Journal of Central South University, 2017, 24(9): 1929–1933.
[8] JANG S W, KIM E S. Enhanced quality factor of wollastonite ($0.9Ca_{0.9}Mg_{0.1}SiO_3$–$0.1CaMgSi_2O_6$) glass-ceramics by heat-treatment method [J]. Materials Research Bulletin, 2015, 67: 239–244.
[9] SALMAN S M, SALAMA S N, ABO-MOSALLAM H A. The crystallization behavior and bioactivity of wollastonite glass-ceramic based on Na_2O-K_2O-CaO-SiO_2-F glass system [J]. Journal of Asian Ceramic Societies, 2015, 48(3): 255–261.
[10] YOON S D, LEE J U, LEE J H, YUN Y H, YOON W J. Characterization of wollastonite glass-ceramics made from waste glass and coal fly ash [J]. Journal of Materials Science & Technology, 2013, 29(2): 149–153.
[11] CANNILLO V, COLMENARES-ANGULO J, LUSVARGHI L, PIERLI F, SAMPATH S. In vitro characterisation of plasma-sprayed apatite/wollastonite glass-ceramic biocoatings on titanium alloy [J]. Journal of the European Ceramic Society, 2009, 29(9): 1665–1677.
[12] MAGALLANES-PERDOMO M, LUKLINSKA Z B, PENA P, AZA A H D, CARRODZGUAS R G, AZA S D. Bone-like forming ability of apatite- wollastonite glass ceramic [J]. Journal of the European Ceramic Society, 2011, 31(9): 1549–1561.
[13] GONG Y, DONGOL R, YATONGCHAI C, WKZN A W, SUNDARAM S K, MEUOTT N P. Recycling of waste amber glass and porcine bone into fast sintered and high strength glass foams [J]. Journal of Cleaner Production, 2016, 112: 4534–4539.
[14] ZHU Meng-guang, JI Ru, LI Zhong-min, WANG Hao, LIU Li-li, ZHANG Zuo-tai. Preparation of glass ceramic foams for thermal insulation applications from coal fly ash and waste glass [J]. Construction & Building Materials, 2016, 112: 398–405.
[15] PAGLIOLICO S L, LO VERSO V R M, TORTA A, GIKAUD M, CANONICO F, LIGI L. A preliminary study on light transmittance properties of translucent concrete panels with coarse waste glass inclusios [J]. Energy Procedia, 2015, 78: 1811–1816.
[16] BINHUSSAIN M A, MARANGONI M, BERNARDO E, COLOMBO P Sintered and glazed glass-ceramics from natural and waste raw materials [J]. Ceramics International, 2014, 40(2): 3543–3551.
[17] PONSOT I, FALCONE R, BERNARDO E. Stabilization of fluorine-containing industrial waste by production of sintered glass-ceramics [J]. Ceramics International, 2013, 39(6): 6907–6915.
[18] ABBASI M, HASHEMI B. Fabrication and characterization of bioactive glass-ceramic using soda-lime-silica waste glass [J]. Materials Science and Engineering C: Materials for Biological Applications, 2014, 37(4): 399–404.
[19] ZHANG Wei-yi, LIU He. A low cost route for fabrication of wollastonite glass-ceramics directly using soda-lime waste glass by reactive crystallization-sintering [J]. Ceramics International, 2013, 39(2): 1943–1949.
[20] ZHANG Wei-yi, GAO Hong, XU Yu. Sintering and reactive crystal growth of diopside-albite glass-ceramics from waste glass [J]. Journal of the European Ceramic Society, 2011, 31(9): 1669–1675.
[21] SI Wei, XU Hua-shen, SUN Ming, DING Chao, ZHANG Wei-yi. Transformation mechanism of fluormica to fluoramphibole in fluoramphibole glass ceramics [J]. Advances in Materials Science and Engineering, 2016, 2016 (7, 8): 1–8.
[22] ZHANG Wei-yi, GAO Hong. Preparation of machinable fluoramphibole glass-ceramic from soda-lime glass and fluormica [J]. International Journal of Applied Ceramic Technology, 2008, 5(4): 412–418.
[23] ZHANG Wei-yi, GAO Hong, LI Bo-yu, JIAO Qi-bin. A novel route for fabrication of machinable fluoramphibole glass-ceramics [J]. Scripta Materialia, 2006, 55(3): 275–278.
[24] YANG H, PREWITT C T. On the crystal structure of pseudowollastonite ($CaSiO_3$) [J]. American Mineralogist, 1999, 84(5, 6): 929–932.
[25] KAYGILI O, YAVUZ H. The effects of gamma irradiation on non-isothermal crystallization kinetics and microhardness of the Li_2O-Al_2O_3-SiO_2 glass-ceramic [J]. Journal of Thermal Analysis & Calorimetry, 2010, 102(2): 681–684.

(Edited by YANG Hua)

中文导读

硅灰石玻璃陶瓷的析晶特性及其析晶热力学和动力学

摘要：将废玻璃粉与钙铝黄长石混合，使用反应析晶烧结法制备了硅灰石玻璃陶瓷。采用 X 射线衍射分析、扫描电镜、能谱、高分辨透射电镜和热分析等方法，研究了硅灰石玻璃陶瓷的析晶特性及其析晶热力学与动力学。结果表明，钙铝黄长石与二氧化硅发生反应，析出硅灰石及氧化铝。该硅灰石晶体为一定长径比的板条状，能起到很好的桥联与补强作用。反应析晶过程中钙铝黄长石的铝离子向玻璃中扩散，玻璃的硅离子向钙铝黄长石中扩散，使具有三维架状结构的钙铝黄长石遭到部分破坏，形成链状结构的硅灰石。析晶热力学及动力学研究结果表明，在较低温度（1173 K）下，添加 20 wt% 钙铝黄长石作为反应析晶促进剂，该析晶反应可自发进行。使用 Kissinger 法计算析晶活化能为 261.99 kJ/mol。制备的大块硅灰石玻璃陶瓷（7.5 cm×7.5 cm）抗压强度可达 251 MPa。

关键词：玻璃陶瓷；析晶热力学；析晶动力学